Intercellular Transportation of Quantum Dots Mediated by Membrane Nanotubes

Kangmin He,[†,§] Wangxi Luo,[‡,§] Yuliang Zhang,[‡] Fei Liu,[†] Da Liu,[‡] Li Xu,[‡] Lei Qin,[†] Chunyang Xiong,[†] Zhizhen Lu,[†] Xiaohong Fang,[‡,*] and Youyi Zhang[†,*]

[†]Academy for Advanced Interdisciplinary Studies and Institute of Vascular Medicine of Third Hospital, Ministry of Education Key Lab of Molecular Cardiovascular Sciences, Peking University, Beijing, 100191, China, and [‡]Beijing National Laboratory for Molecular Sciences, Key Laboratory of Molecular Nanostructures and Nanotechnology, Institute of Chemistry, Chinese Academy of Sciences, Beijing 100190, China. [§]These two authors contributed equally to this work.

ARTICLE

ABSTRACT In this work, we reported that the quantum dot (QD) nanoparticles could be actively transported in the membrane nanotubes between cardiac myocytes. Single particle imaging and tracking of QDs revealed that most QDs moved in a bidirectional mode along the membrane nanotubes with a mean velocity of 1.23 μm/s. The results suggested that QDs moving in the nanotubes were coordinately motivated by molecular motors. It provides new information for the study of intercellular transportation of nanoparticles.

KEYWORDS: quantum dots · membrane nanotubes · intercellular transportation · single particle tracking · molecular motor

Membrane nanotubes, the newly discovered nanotubular structures (50−200 nm in diameter) which mediate membrane continuity between mammalian cells over a long distance, represent a novel biological principle of cell-to-cell communication.[1−3] Membrane nanotubes are different from the well-known filopodial bridges of cells, as they are longer (up to several cell diameters in length), exhibit a seamless and continuous membrane transition to the surface of the connected cells, and hover in the cell medium without attaching to the substrate.[4,5] Since the first report in 2004, membrane nanotubes have been identified between many types of cells, both *in vitro* and *in vivo*.[1,3,6−8] Up to now, much effort has been made to study the cargo transport *via* membrane nanotubes and their physiological implications. Membrane components,[4] Ca^{2+},[9] mitochondria,[3] bacteria,[10] murine leukemia virus,[11] HIV-1[5] and prion[7] were found to be transferred along membrane nanotubes between cells over long distances. However, some small cytoplasmic molecules like calcein were impeded,[6] indicating a mechanism of selective transfer. To date, whether nanoparticles such as quantum dots (QDs) can be transferred along membrane nanotubes is yet unknown.

Semiconductor QDs are a new class of fluorescent nanoparticles which have gained wide applications in molecular imaging and nanomedicine due to their narrow and size-tunable emission spectra, broad absorption profiles, and superior photostability.[12,13] The recent years have witnessed a great success on using QDs for cell and tissue labeling,[14,15] membrane receptors imaging and tracking in live cells,[16,17] siRNA delivery monitoring[18] and most recently for siRNA delivery as a carrier reagent.[19] Considering their increasing applications, it is vital to understand the intracellular and intercellular properties of QDs. Ruan *et al*. examined the cellular uptake and intracellular transport of QDs in live cells by spinning-disk confocal microscopy.[14] They found that QDs modified by the cell-penetrating peptide TAT were internalized by macropinocytosis, and they proposed that the cellular Tat-QDs were actively transported by the molecular machines (such as dyneins) along microtubule tracks. However, the intercellular behavior of QDs was not explored.

In this work, we reported for the first time, the intercellular transport of QDs mediated by membrane nanotubes. Rat cardiac myoblast cells (H9c2 cells) which can form membrane nanotubes were used. Streptavidin-coated CdSe/ZnS QDs were found to be uptaken by the cells. Using advanced single particle imaging and tracking technique, it was observed that the internalized QDs were transported bidirectionally along membrane nanotubes with a mean velocity of 1.23 ± 0.01 μm/s. Further analysis of the velocity of individual QDs suggested that the QDs moving inside membrane nanotubes were cooperatively motivated by molecular motors. The results

*Address correspondence to xfang@iccas.ac.cn, zhangyy@bjmu.edu.cn.

Received for review September 1, 2009 and accepted May 24, 2010.

Published online June 4, 2010.
10.1021/nn1002198

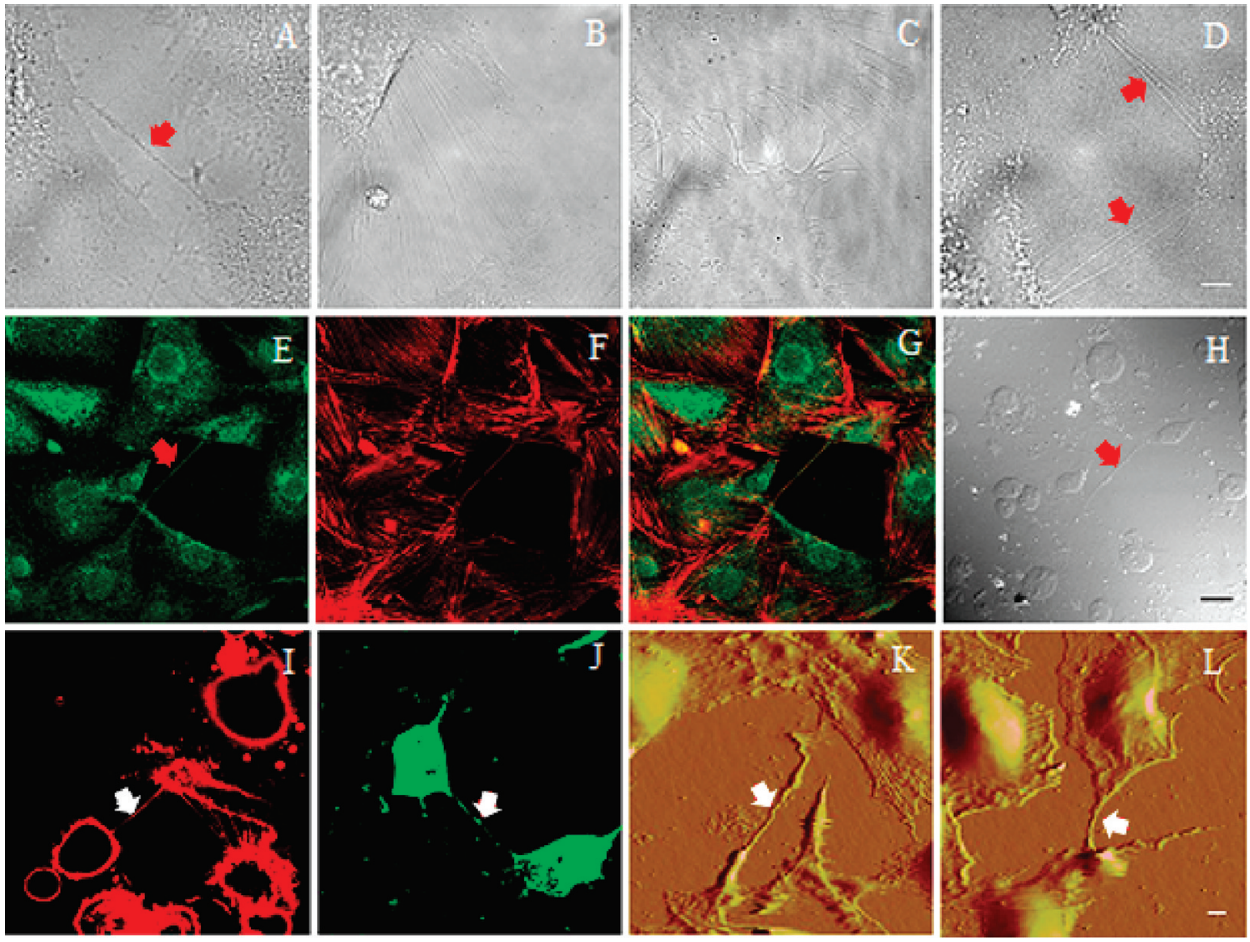

Figure 1. Images of membrane nanotubes (shown by arrows) among the cardiac myoblast H9c2 cells. A single membrane nanotube (A), multiple parallel tubes (B), branched nanotubes (C), and membrane nanotubes network multiple cells (D) were observed. Staining the cells with α-tubulin antibody (E) and rhodamine-conjugated phalloidin (F) indicated that the membrane nanotubes contained both microtubules and F-actins. The overlapped fluorescent image (G) of panels E and F, and the corresponding bright field image (H) were shown. The membrane nanotubes and the connecting cells were stained with membrane dye DiD (I) and cytosolic entity fluorescent probe CellTracker green (J). Typical contact mode deflection images of a membrane nanotube that was pulled apart before completing AFM imaging (K) and an intact membrane nanotube between the cells imaged (L) were shown. Scale bars, 8 μm.

provide new information for the application of QDs in cell imaging and drug delivery. Moreover, monitoring QDs trafficking in membrane nanotubes may offer a new approach to study the working mechanism of molecular motors under physiological conditions.

RESULTS AND DISCUSSION

Membrane Nanotube Formation Between H9c2 Cells. Membrane nanotubes extending from a few micrometers to about 100 μm were observed among cultured H9c2 cells. They can form a single tube (Figure 1A), multiple parallel tubes (Figure 1B), or branched tubes (Figure 1C) between two cells, or occasionally multiple tubes connecting multiple cells (Figure 1D). Although cell-to-cell molecular transport *via* membrane nanotubes from stem cells or endothelial progenitor cells to rat cardiac myocytes has been reported,[3,20] the membrane nanotubes between cardiac myoblast cell lines have neither been observed nor characterized before. By labeling the cells with DiD, a membrane-specific dye, membrane continuity of nanotubes and their connecting cells was shown (Figure 1I). Besides, both nanotubes and the connected cells were stained by cytosolic entity fluorescent probe CellTracker green, indicating the existence of cytosolic entity in membrane nanotubes (Figure 1J). These results confirmed that the membrane nanotubes mediated both membrane and cytosolic connectivity in H9c2 cells, consistent with the membrane nanotubes previously reported in other cell types, such as PC12 cells, macrophages, and CAD cells.[1,7,10] The cytoskeleton component α-tubulin was only reported in the membrane nanotubes between prostate cancer cells or human macrophages;[10,21] we then tested whether the membrane nanotubes between H9c2 cells could be stained with α-tubulin antibody and rhodamine-conjugated phalloidin as well. As shown in Figure 1E−H, both microtubule and F-actin were revealed in the membrane nanotubes we studied.

Membrane nanotubes are sensitive to mechanical stress such as shaking of the culture dishes.[1,3] We tested the strength of membrane nanotubes by imaging with atomic force microscope (AFM), which was mounted on

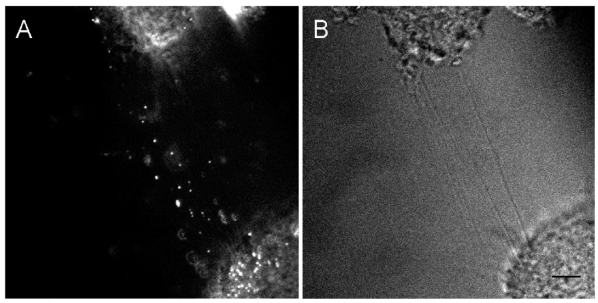

Figure 2. The fluorescence (A) and bright-field imaging (B) of the membrane nanotubes after H9c2 cells were incubated with QDs for 30 min. Scale bars, 8 μm.

the fluorescence microscope. Most membrane nanotubes were so delicate that they were pulled apart before completing the tip scanning (Figure 1K). A few thicker nanotubes which were strong enough to keep the connection between cells during AFM imaging were measured to be about 1 μm in diameter (Figure 1L). As membrane nanotubes hovered in the culture medium and might swing to-and-fro following the moving of the AFM tip, the measured diameters by contact mode AFM were expected to be wider than their actual sizes (hundreds of nanometers).

Transportation of QDs in Membrane Nanotubes. Membrane nanotubes physically connect H9c2 cells over long distances offer a specific and effective way of long distance intercellular communication. To test whether nanoparticles can be transported in the membrane nanotubes, streptavidin-coated CdSe/ZnS QDs, with maximum emission at 605 nm, were incubated with H9c2 cells. Within 30 min, QDs were rapidly internalized into cells (Figure 2A). Previous studies have shown that streptavidin-conjugated CdSe/ZnS QDs could be hardly internalized into cancer cells.[22−25] In our experiment, if we replaced H9c2 cells with HeLa cells, few intracellular QDs were observed in HeLa cells. Therefore, uptake of QDs was cell-specific.

After 30 min incubation with H9c2 cells, many QDs were observed not only inside cells but also located in the connecting membrane nanotubes (Figure 2, Supporting Information, Movie S1). By time-lapse fluorescence imaging, we recorded the movement of QDs in membrane nanotubes. Judging from the blinking property, single QDs inside the nanotubes were identified and tracked for movement analysis.[17]

QDs in membrane nanotubes might originate from direct internalization through the membrane of nanotubes themselves, or traffic from the connecting cells. We confirmed the latter as we observed that several QDs actively moved out from one cell body and consequently moved into the connecting nanotubes, similar to that of GFP-PrPwt vesicles transported between neuronal cells.[7] Figure 3A presented such an example. The QD hovered around the cell periphery for nearly 30 s. Then it moved out of the cell, subsequently moved into the connecting membrane nanotube and headed forward with an accelerated velocity (Figure 3B, Supporting Information, Figure S1 and Movie S2). The corresponding trajectory of the QD was shown in Figure 3C. Besides, we found that some QDs moved completely from one cell to another *via* membrane nanotubes (Supporting Information, Figure S2 and Movie S3). The results suggested the active transportation of QDs in membrane nanotubes.

To reveal whether the QDs in membrane nanotubes were trapped inside any cellular organelle in

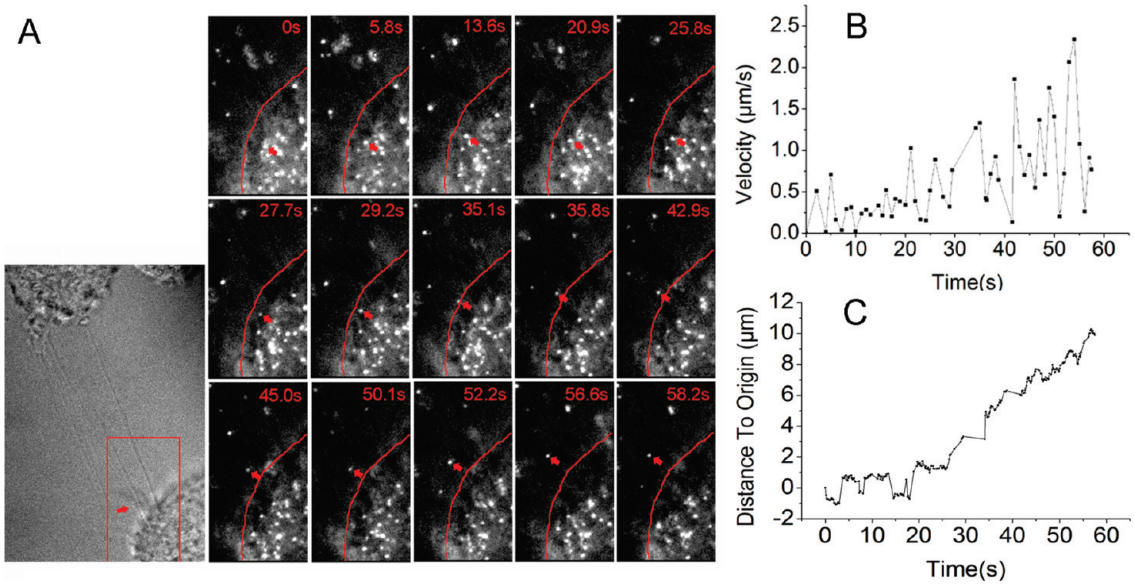

Figure 3. Moving of one QD from the cell body into the connecting membrane nanotube. (A) Time series of the QD movement. The curves marked the cell membrane and the arrows pointed to the QD we studied. The corresponding bright field image was shown in the left corner, with the box drawing the frame of the time series pictures shown in the right and the arrow pointing to the nanotube within which the QD moved along (see also Supporting Information, Movie S2). The velocity (B) and trajectory (C) of the QD were obtained.

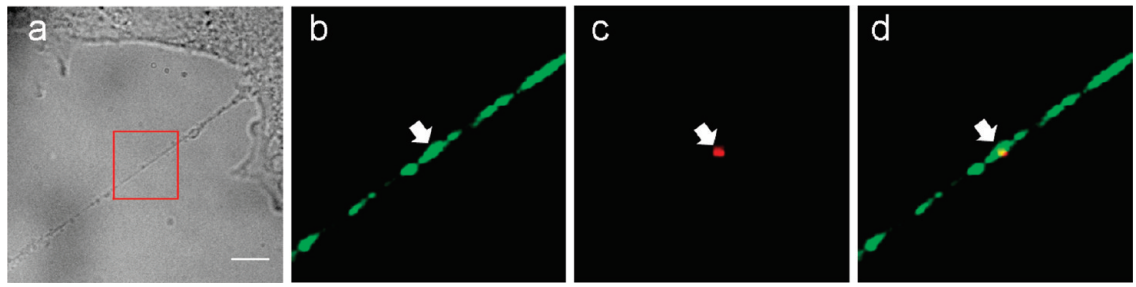

Figure 4. Colocalization of QDs with membrane vehicles inside membrane nanotubes. (a) Bright field of the membrane nanotube and (b−d) the fluorescence images of the boxed region. (b) Green fluorescence of the membrane vehicles shown as swells (arrow), (c) red fluorescence of one QD particle (pointed by arrow), and (d) the overlap of images b and c. Scale bar, 8 μm.

cells as previously reported,[14] H9c2 cells were incubated with QDs for 30 min and then stained with a membrane dye WGA, which was widely used to stain plasma membranes and intracellular vesicles.[26] It was found that the QDs in membrane nanotubes were colocalized or encapsulated in the membrane dye stained vehicles (Figure 4). However, no colocalization of QDs and early endosomes was observed within membrane nanotubes when we stained early endosomes (Supporting Information, Figure S3). This indicated the vehicles for QD transportion in membrane nanotubes were likely to be some cellular organelles other than early endosomes.

Bidirectional Movement of QDs along Membrane Nanotubes. One of the extraordinary features of QDs in membrane nanotubes was their constant shuttling in a bidirectional way along membrane nanotubes. From the movie of QDs moving in the nanotubes (Supporting Information, Movie S1), it was obvious that QDs reversed directions every few seconds. The bidirectional motion has been found to be widely adapted for transportation of many molecular cargos along microtubules in cytoplasm, such as QD-TrkA vesicles, mitochondria, pigment granules, endosomes, lipid-droplets, and viruses.[17,27−29] The bidirectional motion is advantageous in dynamic regulation, error correction, and the establishment of polarized organelle distributions.[28] Recently, vesicles moving inside thick membrane nanotubes between macrophages have been reported as bidirectional as well.[10] In our study, we also found the bidirectional moving of nanoparticles in the membrane nanotubes between cardiac myocytes.

After recording the bidirectional movement of individual QDs for 67.5 s, we calculated their moving distances along the membrane nanotubes from their recording start points to end points. It was found that with the bidirectional moving, more than 80% of QDs actually headed toward one of the connected cells. Figure 5A showed the movement analysis of 11 observed QDs moving between the two cells in Figure 2A (Supporting Information, Movie S1). The majority of QDs (9 of 11 QDs) headed toward the upper left cell which was poor in QDs. Only a few QDs (2 of 11) moved around the original recording start point without a clear direction. For most QDs, they moved more than 4 μm in distance along membrane nanotubes. It seemed that the cells containing less QDs tended to receive QDs from those rich in QDs (Figure 2A, Supporting Information, Figure S2, Movie S1, and Movie S3), thus directed transport of nanoparticles between two connected cells was possible. The QDs concentration in neighboring cells might act as the driving force behind the directional transport by membrane nanotubes. This type of directed transport through bidirectional movement has

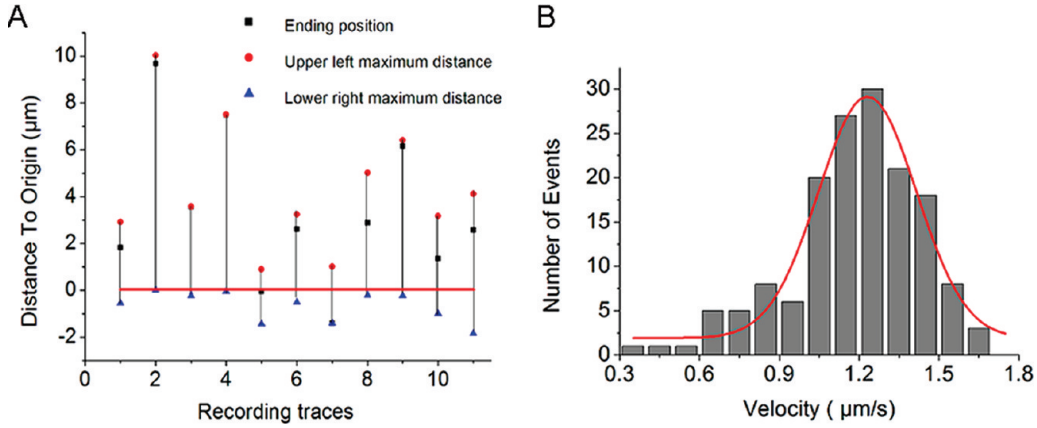

Figure 5. (A) Distance to the original recording start point (the red line, set as zero) of all moving QDs along the membrane nanotubes in Figure 2A. (B) Histogram of velocities of QDs moving along membrane nanotubes (n = 154) (fitting with a Gaussian function, curve).

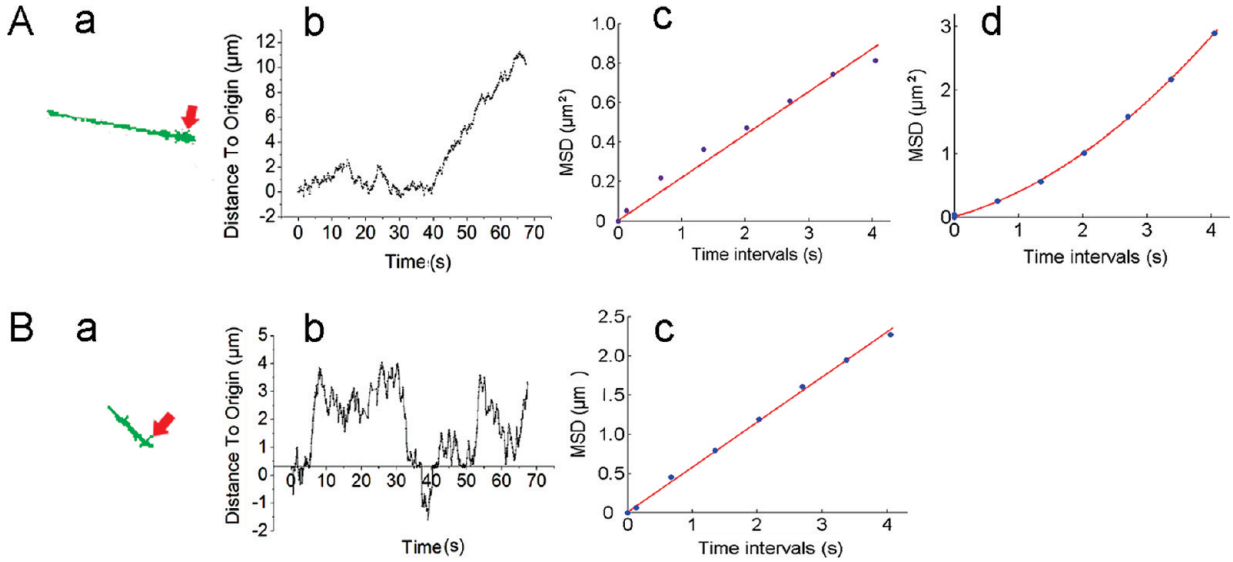

Figure 6. (A) Directed movement of one QD particle within membrane nanotubes (also see Supporting Information, Movie S4). The trajectory (arrow points to the recording start point) (a) and distance (b) to the recording start point of the QDs. Two stages of diffusive movement (before 40 s) and directed movement (after 40 s) were confirmed by the corresponding linear (c) and superlinear (d) MSD-Δ*t* plots. (B) An example showing a moving QD without a clear direction (also see Supporting Information, Movie S5). The trajectory (arrow points the recording start point) (a), distance to the recoding start point (b), and MSD-Δ*t* of the QDs (c) at different times. The curves in panels A,c, A,d, and B,c are the fitting curves with the equation $\rho(t) = v^2t^2 + 2Dt$ (see Materials and Methods for details).

been reported to facilitate virus spread from infected cells to uninfected cells, and organelles exchange between different types of cells.[3,5,7,11,20]

Figure 6A showed an example of the directed movement of one QD particle along the membrane nanotube in detail (Figure 6A,a) (Supporting Information, Movie S4). It was characterized by a backward and forward movement around the original recording start point for nearly 40 s, then speeded up and moved straightforward for more than 12 μm (Figure 6A,b). The two stages of diffusive movement (before 40 s) and directed movement (after 40 s) were confirmed by the corresponding linear (Figure 6A,c) and superlinear (Figure 6A,d) plots of mean squared displacement (MSD) *versus* the time intervals of 0−4 s. The velocity of the QDs kept fluctuating, with a maximum velocity of 4.27 μm/s and minimum of 0.054 μm/s. Another example of the moving QDs without clear direction was represented in Figure 6B (Supporting Information, Movie S5). The linear MSD plot in Figure 6B,c indicated the free Brownian diffusion.[30] The fluorescent blinking property presented by the fluorescence fluctuation of the two particles (Supporting Information, Figure S4) confirmed that they were single nanoparticles.[17]

The speeds of QDs traveling along membrane nanotubes were further quantified. The velocity distribution of 154 individual trajectories of QDs moving in the nanotubes between seven pairs of cells was shown in Figure 5B with the mean velocity of 1.23 ± 0.01 μm/s, which was in agreement with the reported velocity of DiD labeled vesicles running inside membrane nanotubes.[10] As this mean velocity value was similar to that of dyneins or kinesins walking on intracellular microtubules under *in vitro* and *in vivo* conditions,[14,31−34] we suspected that the movement of QDs along intercellular membrane nantoubes might also be mediated by molecular motors on microtubules.

Bidirectional Movement of QDs Driven Coordinately by Multiple Molecular Motors. The observed bidirectional movement and the velocity of QDs all suggested the possibility of their movement mediated by microtubules and microtubular motors. The existence of micro-

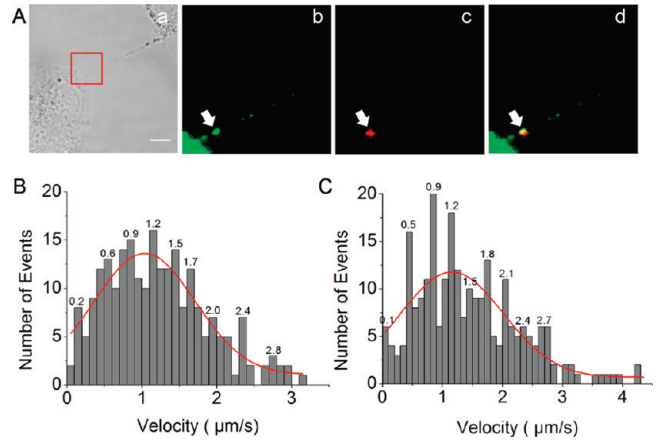

Figure 7. QDs were actively transported by microtubule motors. (A) Colocalization of QDs and kinesin motors within membrane nanotubes: (a) bright field image of a membrane nanotube between two connected cells and (b−d) the fluorescence images of the boxed region; (b) green fluorescence of the kinesin motors stained by kinesin antibody (arrow), (c) red fluorescence of one QD particle (arrow), and (d) the overlap of images b and c. (B) Forward and (C) backward velocity distributions of one typical QD particle in the membrane nanotubes. The mean velocity was 1.04 ± 0.05 μm/s (SD) and 1.16 ± 0.09 μm/s (SD) for the forward and backward movement of the QD, respectively. The curves were the fitting curves with a Gaussian function. Scale bar, 8 μm.

tubules within membrane nanotubes (Figure 1E), together with the evidence of the colocalization of QDs and kinesin motors within membrane nanotubes (Figure 7A) also supported the suspicion. Then, we analyzed the forward and backward velocity of QDs separately from the bidirectional movement. Figure 7B and 7C showed the speed distribution of one representative QD particle moving in the forward and backward directions, respectively. The forward and backward movement displayed similar velocity distribution. The graphs were highly spiked with a constant interval corresponding to 0.3 μm/s for both directions. This distribution pattern was rather similar to what Kural *et al*. reported for peroxisome transport along microtubules inside cells.[34] Kural *et al.* proposed that the constant velocity intervals moving in two directions suggested the cooperative movement driven by kinesins or dyneins along microtubules without any apparent inhibition by the opposite motors. If dynein or kinesin motors operated simultaneously, then any compliance in the motor stalks would cause a degradation of step sizes as well as velocity, as one motor took a step while its competitor was still bound to a microtubule.[34] Therefore, the number of molecular motors can be calculated from the speed distribution. According to their method, since the speed in the minus-end and plus-end by Gaussian fitting to the histograms in Figure 7B and 7C were 1.04 and 1.16 μm/s, respectively, we estimated in our experiment four active dyneins or kinesins molecular motors associated with one QD particle in membrane nanotubes. This value was also in agreement to the previous theoretical estimation that two to five active motors were associated with vesicular cargos moving toward either the plus or minus end of the microtubule.[35] Thus, our results suggested that QDs moving inside membrane nanotubes were motivated by multiple motors working in a cooperative way.

CONCLUSION

We provided the first evidence of intercellular transportation of nanoparticles in membrane nanotubes. The bidirectional movement, velocity distribution of the nanoparticles, and colocalization of QDs with kinesin motors indicated that QD transportation was motivated coordinately by multiple molecular motors. The intercellular transport of QDs along membrane nanotubes implied a new pathway for QD secretion from cells, besides the reported secretion pathways such as excytosis and vesicle shedding for nanoparticles.[14,36]

Membrane nanotubes were observed not only in cultured monolayer cells, but also *in vivo* in the mice corneal stroma and three-dimensional matrix cultured cells as well.[5,8] Up to now, little is known about the molecular basis of membrane nanotubes formation. Only recently, a mammalian protein, M-Sec, was reported as a key regulator of membrane nanotube formation.[37] The physiological implications of membrane nanotubes have been investigated including their roles in important biological processes like embryogenesis, immune defense, transfer of pathogens as well as cancer development.[4,38] The study of intercellular transport of QDs is expected to be of great interest in the further development of QDs as cellular imaging probes and therapeutic reagents. For example, by microinjecting therapeutic molecule conjugated QDs to the carrier cells, therapeutic molecules can be transferred to targeted cells by membrane nanotubes for noninvasive cell therapy.

Moreover, the bidirectional movement of QDs in microtubule-containing membrane nanotubes provides vivid and long-term observations of how microtubule motors work. QDs have been used to track the motion of an individual kinesin motor *in vitro* with 300 μs time resolution and 1.5 nm spatial precision, demonstrating the ability of QDs to probe the operation of an individual motor protein in living cells.[31,39] As membrane nanotubes are advantageous in relatively simple environments, monitoring QDs moving in membrane nanotubes represents a new approach to study the molecular motors under physiological conditions with high spatial and temporal resolution, and long-distance observation avoiding interference from complex cytoplasm.

MATERIALS AND METHODS

Cell Culture and QDs Incubation. Rat cardiac myoblast H9c2 cells were cultured in Dulbecco's modified Eagle's medium (DMEM, Gibco) supplemented with 10% fetal bovine serum (Hyclone) at 37 °C in a 5% CO_2 atmosphere. Cells were plated in a 35 mm glass-bottom dish (Shengyou Biotechnology, China) for 24−40 h prior to membrane nanotubes observation. The 1 nM streptavidin-conjugated CdSe/ZnS QDs (Molecular Probes, Qdot 605 streptavidin conjugate) were incubated with H9c2 cells for 30 min before observation.

Fluorescence Microscopy of the Stained Cells and Membrane Nanotubes. 1,1′-Dioctadecyl-3,3,3′,3′-tetramethylindodicarbocyanine perchlorate (DiD) (Molecular Probes), CellTracker green (Molecular Probes), and WGA Alexa Fluor 488 conjugate (Molecular Probes) were used to stain the live H9c2 cells. For cytoskeleton, early endosomes, and kinesin staining, H9c2 cells were washed in phosphate-buffered saline (PBS), permeabilized in PBS containing 0.5% Triton X-100 for 10 min, and fixed with 4% formaldehyde in PBS for 30 min at room temperature. Purified mouse anti-EEA1 (BD Transduction Laboratories) and DyLight 488-conjugated goat anti-mouse IgG (Jackson ImmunoResearch) (Molecular Probes) were used to stain early endosomes. Microtubule was stained using the rabbit anti human TUBA1 polyclonal antibody (Proteintech Group, Inc.). F-actin was labeled with rhodamine phalloidin (Molecular Probes). Kinesin was stained using the antikinesin antibody (Abcom).

The cells stained with different fluorescent dyes were imaged by the confocal microscope (FluoView FV1000 Olympus, Japan) with a 100 × /1.40NA oil objective and excitation wavelengths at 488 or 559 nm.

AFM Imaging. AFM images were performed with Bioscope (Veeco, Santa Barbara, CA) operating in the contact mode in liquid. Silicone nitride cantilevers with spring constants of about 0.06 N/m were used. The topography and deflection images were obtained with 256 × 256 pixels^2 at line rates of 0.5 Hz.

Imaging of QDs Transportation in Membrane Nanotubes. Fluorescence imaging of QDs was performed with the wide-field fluorescence microscope equipped with a 100×/1.45NA Plan Apochromat objective (Olympus, Japan) and a 14-bit back-illuminated electron-multiplying charge-coupled device camera (EMCCD) (Andor iXon DU-897 BV). The microscope was also equipped with a cell incubation system (INU-ZIL-F1, TOKAI HIT) which ensured living cell imaging at 37 °C in 5% CO_2. QDs were excited at 488-nm by an argon laser (Melles Griot, Carlsbad, CA). Movies were acquired at a frame rate of 10 Hz using MetaMorph software (Molecular Device).

QDs Trajectory and MSD Calculation. Single-particle tracking of QDs was analyzed with MetaMorph software (Molecular Device). The position of each QD vesicle was determined by locating the center of the fluorescence spots through a two-dimensional Gaussian fit.

Mean squared displacement (MSD) was calculated for each time interval Δt ($\Delta t = n\delta t$, δt was 675 ms in our study) over a trajectory by the equation:[40]

$$\mathrm{MSD}(n\delta t) = \frac{1}{N-1-n}\sum_{i=1}^{N-1-n}\{[x(i\delta t + n\delta t) - x(i\delta t)]^2 + [y(i\delta t + n\delta t) - y(i\delta t)]^2\}$$

where $(x(i\delta t + n\delta t), y(i\delta t + n\delta t))$ is the spot position at a time interval Δt after starting at the position $(x(i\delta t), y(i\delta t))$. N is the total number of image frames, and n and i are integers, with n determining the time increment.

Plots of the MSD against the time interval were fit over the first several time intervals to the equation: $\mathrm{MSD}[\rho(t)] = 2D\Delta t + V^2\Delta t^2$, where V is the mean velocity estimated by fitting $\rho(t)$ with $\rho(t) = 2D\Delta t + V^2\Delta t^2$ and D is the random, diffusive contribution.[41]

Acknowledgment. This work was supported by the National Basic Research Program of China (2007CB935601), National Natural Science Foundation of China (90713024, 30821001, 20821003), Chinese Academy of Sciences and the Key grant Project of Chinese Ministry of Education (307001).

Supporting Information Available: Histograms of velocities of the QD in Figure 3 (Figure S1). QDs exchanged between two adjacent cells by passing completely from one cell to another *via* membrane nanotubes (Figure S2). QDs were scarcely colocalized with early endosomes in cells and membrane nanotubes (Figure S3). The fluorescence intensity fluctuations of the QDs in Figure 6A and Figure 6B (Figure S4). Imaging of QDs constantly shuttling bidirectionally along several parallel membrane nanotubes between H9c2 cells (Movie S1). Imaging of the QD particle moved out of a cell and subsequently moved into the connected membrane nanotube (Movie S2). Transportation of the QDs particle between two adjacent cells *via* membrane nanotubes (Movie S3). Examples of moving QDs with and without clear directions in membrane nanotubes (Movie S4 and Movie S5). This material is available free of charge *via* the Internet at http://pubs.acs.org.

REFERENCES AND NOTES

1. Rustom, A.; Saffrich, R.; Markovic, I.; Walther, P.; Gerdes, H. H. Nanotubular Highways for Intercellular Organelle Transport. *Science* **2004**, *303*, 1007–1010.
2. Gerdes, H. H.; Bukoreshtliev, N. V.; Barroso, J. F. V. Tunneling Nanotubes: A New Route for the Exchange of Components Between Animal Cells. *FEBS Lett.* **2007**, *581*, 2194–2201.
3. Koyanagi, M.; Brandes, R. P.; Haendeler, J.; Zeiher, A. M.; Dimmeler, S. Cell-to-Cell Connection of Endothelial Progenitor Cells with Cardiac Myocytes by Nanotubes: A Novel Mechanism for Cell Fate Changes. *Circ. Res.* **2005**, *96*, 1039–1041.
4. Gerdes, H. H.; Carvalho, R. N. Intercellular Transfer Mediated by Tunneling Nanotubes. *Curr. Opin. Cell Biol.* **2008**, *20*, 470–475.
5. Sowinski, S.; Jolly, C.; Berninghausen, O.; Purbhoo, M. A.; Chauveau, A.; Köhler, K.; Oddos, S.; Eissmann, P.; Brodsky, F. M.; Hopkins, C.; *et al.* Membrane Nanotubes Physically Connect T Cells Over Long Distances Presenting a Novel Route for HIV-1 Transmission. *Nat. Cell Biol.* **2008**, *10*, 211–219.
6. Davis, D. M.; Sowinski, S. Membrane Nanotubes: Dynamic Long-Distance Connections between Animal Cells. *Nat. Rev. Mol. Cell Biol.* **2008**, *9*, 431–436.
7. Gousset, K.; Schiff, E.; Langevin, C.; Marijanovic, Z.; Caputo, A.; Browman, D. T.; Chenouard, N.; de Chaumont, F.; Martino, A.; Enninga, J.; *et al.* Prions Hijack Tunnelling Nanotubes for Intercellular Spread. *Nat. Cell Biol.* **2009**, *11*, 328–336.
8. Chinnery, H. R.; Pearlman, E.; McMenamin, P. G. Cutting Edge: Membrane Nanotubes *in Vivo*: A Feature of MHC Class II$^+$ Cells in the Mouse Cornea. *J. Immunol.* **2008**, *180*, 5779–5783.
9. Watkins, S. C.; Salter, R. D. Functional Connectivity Between Immune Cells Mediated by Tunneling Nanotubules. *Immunity* **2005**, *23*, 309–318.
10. Onfelt, B.; Nedvetzki, S.; Benninger, R. K.; Purbhoo, M. A.; Sowinski, S.; Hume, A. N.; Seabra, M. C.; Neil, M. A.; French, P. M.; Davis, D. M. Structurally Distinct Membrane Nanotubes between Human Macrophages Support Long-Distance Vesicular Traffic or Surfing of Bacteria. *J. Immunol.* **2006**, *15*, 8476–8483.
11. Sherer, N. M.; Lehmann, M. J.; Jimenez-Soto, L. F.; Horensavitz, C.; Pypaert, M.; Mothes, W. Retroviruses Can Establish Filopodial Bridges for Efficient Cell-to-Cell Transmission. *Nat. Cell Biol.* **2007**, *9*, 243–244.
12. Duan, H. W.; Nie, S. M. Cell-Penetrating Quantum Dots Based on Multivalent and Endosome-Disrupting Surface Coatings. *J. Am. Chem. Soc.* **2007**, *129*, 3333–3338.
13. Ko, M. H.; Kim, S.; Kang, W. J.; Lee, J. H.; Kang, H.; Moon, S. H.; Hwang, D. W.; Ko, H. Y.; Lee, D. S. *In vitro* Derby Imaging of Cancer Biomarkers Using Quantum Dots. *Small* **2009**, *5*, 1207–1212.
14. Ruan, G.; Agrawal, A.; Marcus, A. I.; Nie, S. Imaging and Tracking of TAT Peptide-Conjugated Quantum Dots in Living Cells: New Insights into Nanoparticle Uptake, Intracellular Transport, and Vesicle Shedding. *J. Am. Chem. Soc.* **2007**, *129*, 14759–14766.
15. Yong, K. T.; Ding, H.; Roy, I.; Law, W. C.; Bergey, E. J.; Maitra, A.; Prasad, P. N. Imaging Pancreatic Cancer Using Bioconjugated InP Quantum Dots. *ACS Nano* **2009**, *3*, 502–510.
16. Gussin, H. A.; Tomlinson, I. D.; Little, D. M.; Warnement, M. R.; Qian, H.; Rosenthal, S. J.; Pepperberg, D. R. Binding of Muscimol-Conjugated Quantum Dots to $GABA_C$ Receptors. *J. Am. Chem. Soc.* **2006**, *128*, 15701–15713.
17. Sundara, R. S.; Vu, T. Q. Quantum Dots Monitor TrkA Receptor Dynamics in the Interior of Neural PC12 Cells. *Nano Lett.* **2006**, *6*, 2049–2059.
18. Chen, A. A.; Derfus, A. M.; Khetani, S. R.; Bhatia, S. N. Quantum Dots to Monitor RNAi Delivery and Improve Gene Silencing. *Nucleic Acids Res.* **2005**, *33*, e190.
19. Yezhelyev, M. V.; Qi, L.; O'Regan, R. M.; Nie, S.; Gao, X. Proton-Sponge Coated Quantum Dots for siRNA Delivery and Intracellular Imaging. *J. Am. Chem. Soc.* **2008**, *130*, 9006–9012.
20. Plotnikov, E. Y.; Khryapenkova, T. G.; Vasileva, A. K.; Marey, M. V.; Galkina, S. I.; Isaev, N K.; Sheval, E. V.; Polyakov, V. Y.; Sukhikh, G. T.; Zorov, D. B. Cell-to-Cell Cross-Talk Between Mesenchymal Stem Cells and Cardiomyocytes in Co-culture. *J. Cell Mol. Med.* **2008**, *12*, 1622–1631.
21. Vidulescu, C.; Clejan, S.; O'Connor, K. C. Vesicle Traffic Through Intercellular Bridges in DU 145 Human Prostate Cancer Cells. *J. Cell Mol. Med.* **2004**, *8*, 388–396.
22. Wu, X.; Liu, H.; Liu, J.; Haley, K. N.; Treadway, J. A.; Larson,

J. P.; Ge, N.; Peale, F.; Bruchez, M. P. Immunofluorescent Labeling of Cancer Marker Her2 and Other Cellular Targets with Semiconductor Quantum Dots. *Nat. Biotechnol.* **2003**, *21*, 32–33.
23. Howarth, M.; Takao, K.; Hayashi, Y.; Ting, A. Y. Targeting Quantum Dots to Surface Proteins in Living Cells with Biotin Ligase. *Proc. Natl. Acad. Sci. U.S.A.* **2005**, *102*, 7583–7588.
24. Smith, A. M.; Duan, H.; Mohs, A. M.; Nie, S. Bioconjugated Quantum Dots for *in Vivo* Molecular and Cellular Imaging. *Adv. Drug Delivery Rev.* **2008**, *60*, 1226–1240.
25. Chen, B.; Liu, Q. L.; Zhang, Y. L.; Xu, L.; Fang, X. H. Transmembrane Delivery of the Cell-Penetrating Peptide Conjugated Semiconductor Quantum Dots. *Langmuir* **2008**, *24*, 11866–11871.
26. Kanazawa, T.; Takematsu, H.; Yamamoto, A.; Yamamoto, H.; Kozutsumi, Y. Wheat Germ Agglutinin Stains Dispersed Postgolgi Vesicles after Treatment with the Cytokinesis Inhibitor Psychosine. *J. Cell Physiol.* **2008**, *215*, 17–25.
27. Gross, S. P.; Welte, M. A.; Block, S. M.; Wieschaus, E. F. Coordination of Opposite-Polarity Microtubule Motors. *J. Cell Biol.* **2002**, *156*, 715–724.
28. Welte, M. A. Bidirectional Transport Along Microtubules. *Curr. Biol.* **2004**, *4*, R525–537.
29. Müller, M. J.; Klumpp, S.; Lipowsky, R. Tug-of-war as a Cooperative Mechanism for Bidirectional Cargo Transport by Molecular Motors. *Proc. Natl. Acad. Sci. U.S.A.* **2008**, *105*, 4609–4614.
30. Dahan, M.; Lévi, S.; Luccardini, C.; Rostaing, P.; Riveau, B.; Triller, A. Diffusion Dynamics of Glycine Receptors Revealed by Single-Quantum Dot Tracking. *Science* **2003**, *302*, 442–445.
31. King, S. J.; Schroer, T. A. Dynactin Increases the Processivity of the Cytoplasmic Dynein Motor. *Nat. Cell Biol.* **2000**, *2*, 20–24.
32. Nan, X.; Sims, P. A.; Chen, P.; Xie, X. S. Observation of Individual Microtubule Motor Steps in Living Cells with Endocytosed Quantum Dots. *J. Phys. Chem. B* **2005**, *109*, 24220–24224.
33. Nishiura, M.; Kon, T.; Shiroguchi, K.; Ohkura, R.; Shima, T.; Toyoshima, Y. Y.; Sutoh, K. A Single-Headed Recombinant Fragment of Dictyostelium Cytoplasmic Dynein Can Drive the Robust Sliding of Microtubules. *J. Biol. Chem.* **2004**, *279*, 22799–22802.
34. Kural, C.; Kim, H.; Syed, S.; Goshima, G.; Gelfand, V. I.; Selvin, P. R. Kinesin and Dynein Move a Peroxisome *in Vivo*: A Tug-of-War or Coordinated Movement. *Science* **2005**, *308*, 1469–14672.
35. Caviston, J. P.; Holzbaur, E. L. Microtubule Motors at the Intersection of Trafficking and Transport. *Trends Cell Biol.* **2006**, *16*, 530–537.
36. Panyam, J.; Labhasetwar, V. Dynamics of Endocytosis and Exocytosis of Poly(D,L-lactide-*co*-glycolide) Nanoparticles in Vascular Smooth Muscle Cells. *Pharm. Res.* **2003**, *20*, 212–220.
37. Hase, K.; Kimura, S.; Takatsu, H.; Ohmae, M.; Kawano, S.; Kitamura, H.; Ito, M.; Watarai, H.; Hazelett, C. C.; Yeaman, C.; Ohno, H. M-Sec Promotes Membrane Nanotube Formation by Interacting with Ral and the Exocyst Complex. *Nat. Cell Biol.* **2009**, *11*, 1427–1432.
38. Onfelt, B.; Purbhoo, M. A.; Nedvetzki, S.; Sowinski, S.; Davis, D. M. Long-Distance Calls between Cells Connected by Tunneling Nanotubules. *Sci. STKE* **2005**, *313*, pe55.
39. Courty, S.; Luccardini, C.; Bellaiche, Y.; Cappello, G.; Dahan, M. Tracking Individual Kinesin Motors in Living Cells Using Single Quantum-Dot Imaging. *Nano Lett.* **2006**, *6*, 1491–1495.
40. Ma, X. Y.; Wang, Q.; Jiang, Y. X.; Xiao, Z. Y.; Fang, X. H.; Chen, Y. G. Lateral Diffusion of TGF-b Type I Receptor Studied by Single-Molecule Imaging. *Biochem. Bioph. Res. Commun.* **2007**, *356*, 67–71.
41. Okada, Y.; Hirokawa, N. A Processive Single-Headed Motor: Kinesin Superfamily Protein KIF1A. *Science* **1999**, *283*, 1152–1157.